Vector chirality for effective total momentum $J_{\rm eff}$ in a nonfrustrated Mott insulator: Effects of strong spin-orbit coupling and broken inversion symmetry

Naoya Arakawa*
Center for Emergent Matter Science (CEMS), RIKEN, Wako, Saitama 351-0198, Japan
(Dated: November 10, 2016)

I propose the emergence of the spin-orbital-coupled vector chirality in a non-frustrated Mott insulator with the strong spin-orbit coupling due to *ab*-plane's inversion-symmetry (IS) breaking. I derive the superexchange interactions for a t_{2g}-orbital Hubbard model on a square lattice with the strong spin-orbit coupling and the IS-breaking-induced hopping integrals, and explain the microscopic origins of the Dzyaloshinsky-Moriya (DM) -type and the Kitaev-type interactions. Then, by adopting the mean-field approximation to a minimal model including only the Heisenberg-type and the DM-type nearest-neighbor interactions, I show that the IS breaking causes the spin-orbital-coupled chirality as a result of stabilizing the screw state. I also highlight the limit of the hard-pseudospin approximation in discussing the stability of the screw states in the presence of both the DM-type and the Kitaev-type interactions, and discuss its meaning. I finally discuss the effects of tetragonal crystal field and $J_{\rm eff}=\frac{3}{2}$ states, and the application to the iridates near the [001] surface of Sr_2IrO_4 and the interface between Sr_2IrO_4 and $Sr_3Ir_2O_7$.

arXiv:1604.05867v3 [cond-mat.str-el] 8 Nov 2016

I. INTRODUCTION

The spin chirality is a key concept in condensed-matter physics. That is categorized as either vector-type one, $\boldsymbol{S_i}\times\boldsymbol{S_j}$, or scalar-type one, $\boldsymbol{S_i}\cdot(\boldsymbol{S_j}\times\boldsymbol{S_k})$. One of the former's drastic effects is to generate the electric polarization in multiferroic materials such as $TbMnO_3$[1–4]; for the latter, its drastic effect is to cause the anomalous-Hall effect in a frustrated system such as $Pr_2Ir_2O_7$[5,6]. In addition to those, the spin chirality is related to skyrmion physics[7] and heavy-fermion physics[8].

There are two mechanisms for realizing the spin chirality. One arises from the Dzyaloshinsky-Moriya(DM)-type antisymmetric exchange interaction[9,10] such as $\sum_{i,j}\boldsymbol{D_{i,j}}\cdot(\boldsymbol{S_i}\times\boldsymbol{S_j})$ with $\boldsymbol{D_{i,j}}=-\boldsymbol{D_{j,i}}$. In the system in which inversion symmetry (IS) is broken due to lattice distortion, such DM-type interaction appears as a result of the combination effects of the onsite spin-orbit coupling (SOC), the kinetic exchange, and the IS breaking[10]; the DM-type interaction induces the spin vector chirality. This mechanism works in α-Fe_2O_3, for example[10]. The other arises from the competition[11] between the Heisenberg-type symmetric exchange interactions such as $\sum_{i,j}J_{i,j}\boldsymbol{S_i}\cdot\boldsymbol{S_j}$ with $J_{i,j}=J_{j,i}$; this does not need lattice origin's IS breaking. Its example is MnO_2[11]: in a body-centered unit cell the Heisenberg-type interactions between the nearest-neighbor (NN) sites along the c axis compete with others between the body center and each vertex; this competition results in stabilizing a screw state, where the spin vector chirality becomes finite.

Although the understanding of the spin chirality has been developed, the chirality of another degree of freedom is unsatisfactorily understood. For example, we little understand the chirality of the orbital, although its possibility may be suggested by the close similarities between the spin and the orbital about orders and fluctuations[12]. Since the orbital degree of freedom of an electron describes the anisotropy of its spatial distribution, the understanding of the chirality of the orbital may open a new possibility of utilizing the chirality of the anisotropic spatial distribution of electrons/holes. Although there are several studies related to the chirality of the orbital, these focused on the frustrated iridates[13–18], the Ir oxides with the geometric frustration of the symmetric exchange interactions. Since the frustration tends to develop the strong fluctuations, it is difficult to realize the chirality of the orbital as a result of the order; if it is realized, it may be easily broken by a small perturbation because such perturbation is sufficient to stabilize another competed state. Thus, the nonfrustrated system may be better for studies towards realizing the chirality related to the orbital and utilizing and controlling it. However, it has been unclear whether the chirality related to the orbital is realized in the nonfrustrated system with the strong SOC because of lattice origin's IS breaking, although the realization may be suggested by the analogy with the case of the spin chirality in a nonfrustrated system with the weak SOC. Thus, we should clarify the possibility of the chirality related to the orbital in a non-frustrated system with the strong SOC in the presence of the IS breaking.

Here I propose that a nonfrustrated Mott insulator with the strong SOC gains the spin-orbital-coupled vector chirality by introducing the IS breaking on an *ab* plane due to the DM-type interactions for the spin-orbital-coupled degree of freedom[19,20], $\boldsymbol{J_i}=\boldsymbol{S_i}-\boldsymbol{L_i}$ for $J_{\rm eff}=1/2$. Focusing on the essential effects of the IS breaking on the low-energy physics of a quasi-two-dimensional insulating iridate, I derive the superexchange interactions for a t_{2g}-orbital Hubbard model with the strong SOC on a square lattice without *ab*-plane's IS, and explain why the IS breaking leads to the DM-type and the Kitaev-type[21] interactions. Then, by using the mean-field approximation, I show the emergence of the spin-orbital-coupled vector chirality in a minimal model with only the Heisenberg-type and the DM-type NN interactions as a result of stabilizing the screw state. Although even in the presence of the anisotropic terms such

as the Kitaev-type interactions the screw state gives the lowest energy, the hard-pseudospin constraints are violated. This suggests the limit of the hard-pseudospin approximation in discussing the stability of the screw states in the presence of both the DM-type and the Kitaev-type interactions. I finally discuss the validity of the treatment of effects of tetragonal crystal field and the $J_{\rm eff} = \frac{3}{2}$ states, and a possibility of the spin-orbital-coupled vector chirality near the [001] surface of Sr_2IrO_4 and the interface between Sr_2IrO_4 and $Sr_3Ir_2O_7$. Hereafter we set $\hbar = 1$ and choose the lattice constants as unity.

II. METHOD

A. Model

We use a t_{2g}-orbital Hubbard model with the onsite SOC on a square lattice as an effective model of a quasi-two-dimensional iridate, and treat the effects of the IS breaking on an ab plane as the NN hoppings[22,23] between the d_{xy} and d_{yz} orbitals along the x direction, and between the d_{xy} and d_{xz} orbitals along the y direction. (Such treatment is appropriate for a t_{2g}-orbital system, and its applicability is wider than a single-orbital Rashba model[23].) Namely, the Hamiltonian becomes

$$\hat{H} = \hat{H}_{\rm even} + \hat{H}_{LS} + \hat{H}_{\rm int} + \hat{H}_{\rm odd}, \tag{1}$$

where $\hat{H}_{\rm even}$ represents the kinetic energy,

$$\hat{H}_{\rm even} = \sum_{\boldsymbol{i},\boldsymbol{j}} \sum_{a,b} \sum_{s} t^{\rm (even)}_{ab;\boldsymbol{ij}} \hat{c}^{\dagger}_{\boldsymbol{i}as} \hat{c}_{\boldsymbol{j}bs}, \tag{2}$$

with site indices, $\boldsymbol{i}$ and $\boldsymbol{j}$, for N sites, orbital indices, $a, b = d_{xz}, d_{yz}, d_{xy}$, a spin index, $s = \uparrow, \downarrow$, and even-mirror hopping integrals, the hopping integrals even about ab-plane's mirror symmetry, given in Fig. 1; $\hat{H}_{LS}$ the onsite SOC,

$$\hat{H}_{LS} = (-\lambda_{LS}) \sum_{\boldsymbol{i}} \sum_{a,b} \sum_{s,s'} (\boldsymbol{l_i} \cdot \boldsymbol{s_i})_{asbs'} \hat{c}^{\dagger}_{\boldsymbol{i}as} \hat{c}_{\boldsymbol{i}bs'}, \tag{3}$$

with the standard matrix elements $(\boldsymbol{l_i} \cdot \boldsymbol{s_i})_{asbs'}$ (e.g., see Ref. 23); $\hat{H}_{\rm int}$ the multiorbital Hubbard interactions,

$$\hat{H}_{\rm int} = \sum_{\boldsymbol{i}} \sum_{a,b} \hat{c}^{\dagger}_{\boldsymbol{i}a\uparrow} \hat{c}^{\dagger}_{\boldsymbol{i}a\downarrow} [U\delta_{b,a} + J'(1-\delta_{b,a})] \hat{c}_{\boldsymbol{i}b\downarrow} \hat{c}_{\boldsymbol{i}b\uparrow}$$
$$+ \sum_{\boldsymbol{i}} \sum_{a,b(<a)} \sum_{s,s'} \hat{c}^{\dagger}_{\boldsymbol{i}as} \hat{c}^{\dagger}_{\boldsymbol{i}bs'} [U' \hat{c}_{\boldsymbol{i}bs'} \hat{c}_{\boldsymbol{i}as} - J_{\rm H} \hat{c}_{\boldsymbol{i}bs} \hat{c}_{\boldsymbol{i}as'}]; \tag{4}$$

$\hat{H}_{\rm odd}$ the Hamiltonian induced by the IS breaking[22,23],

$$\hat{H}_{\rm odd} = \sum_{\boldsymbol{i},\boldsymbol{j}} \sum_{a,b} \sum_{s} t^{\rm (odd)}_{ab;\boldsymbol{ij}} \hat{c}^{\dagger}_{\boldsymbol{i}as} \hat{c}_{\boldsymbol{j}bs}, \tag{5}$$

with odd-mirror hopping integral, the hopping integral odd about ab-plane's mirror symmetry, given in Fig. 1.

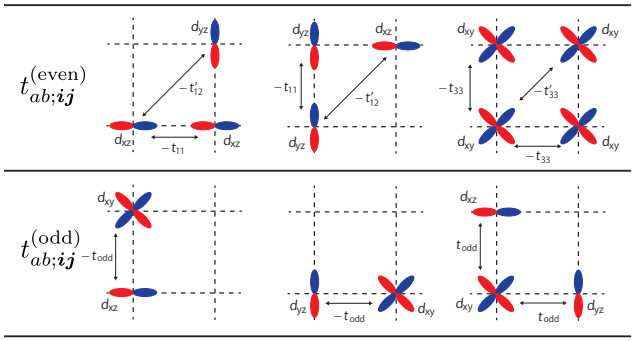

FIG. 1: Schematic pictures of finite $t^{\rm (even)}_{ab;\boldsymbol{ij}}$ and $t^{\rm (odd)}_{ab;\boldsymbol{ij}}$ on a square lattice. The NN hoppings arise from the indirect ones through the $2p$ orbitals of an O ion, and the next-NN hoppings arise from the direct ones.

In our Hamiltonian, we neglect the tetragonal crystal field; the validity will be discussed in Sec. IV. In the analyses, we consider a hole per site because the iridates have the $(t_{2g})^5$-electron configuration[19], equivalent to the $(t_{2g})^1$-hole configuration.

Before the derivation of the low-energy superexchange interactions, I briefly validate the appearance of the odd-mirror hopping integral in the absence of ab-plane's IS. For that purpose, it would be better to begin with the symmetrical properties of the hopping integrals permissible in a square lattice with ab-plane's IS. In the presence of ab-plane's IS, the permissible hopping integrals for the t_{2g} orbitals should be even about z. Furthermore, the permissible hopping integrals along the x and y directions should be even about y and even about x, respectively. Actually, those properties hold for all the hopping integrals of $\hat{H}_{\rm even}$ because the wave functions of the d_{xz}, d_{yz}, and d_{xy} orbitals behave like xz, yz, and xy, respectively, in symmetrical operations; e.g., the NN hopping integral of the d_{xz} orbital along the x direction, behaving like $xz \cdot xz = x^2y^0z^2$, is even about y and z. Then, in the absence of ab-plane's IS, the hopping integrals odd about z, the odd-mirror hopping integrals, become permissible. As a result, the NN hopping integral between the d_{yz} and the d_{xy} orbitals along the x direction is possible because that behaves like $yz \cdot xy = x^1y^2z^1$, which is odd about z and even about y. In addition, the NN hopping integral between the d_{xz} and the d_{xy} orbitals along the y direction is possible. However, the NN hopping integral either between the d_{xz} and the d_{xy} orbitals along the x direction or between the d_{yz} and the d_{xy} orbitals along y direction is prohibited even in the absence of ab-plane's IS. This is because the former is odd about y and the latter is odd about x, and because ab-plane's IS breaking does not affect the symmetrical properties about x and y. The above explanations are the reason why ab-plane's IS breaking induces the odd-mirror hopping integrals. Those hopping integrals are not only odd mirror but also odd parity because the IS breaking considered is the same at each site, i.e. its effects are uniform.

B. Low-energy superexchange interactions

To understand the low-energy physics of $\hat{H}$, we derive the superexchange interactions[24,25] in a strong-correlation limit. Here I will show the result for $J' = J_{\rm H} = 0$ and $U' = U$ in $U, U' \gg \lambda_{LS} \gg |t^{(\rm even)}_{ab;\boldsymbol{ij}}|, |t^{(\rm odd)}_{ab;\boldsymbol{ij}}|$[15,17] in order to focus on the essential effects of the IS breaking as simply as possible. Its effects on the superexchange interactions remain qualitatively the same as the case for $J' > 0$, $J_{\rm H} > 0$, and $U' < U$ (see Appendix A). Including the effects of $\hat{H}_{LS}$ as the formation of the $J = \frac{1}{2}$ states[17], rewriting $\hat{H}_{\rm int}$ in terms of the irreducible representations of the intermediate states[26], treating $\hat{H}_{\rm even} + \hat{H}_{\rm odd}$ in the second-order perturbation, and setting $J' = J_{\rm H} = 0$ and $U' = U$, we obtain an effective Hamiltonian (for more details see Appendix A):

$$\hat{H}_{\rm eff} = J_1 \sum_{\langle \boldsymbol{i},\boldsymbol{j}\rangle} \hat{\boldsymbol{J}}_{\boldsymbol{i}} \cdot \hat{\boldsymbol{J}}_{\boldsymbol{j}} + J_2 \sum_{\langle\langle \boldsymbol{i},\boldsymbol{j}\rangle\rangle} \hat{\boldsymbol{J}}_{\boldsymbol{i}} \cdot \hat{\boldsymbol{J}}_{\boldsymbol{j}} + D \sum_{\langle \boldsymbol{i},\boldsymbol{j}\rangle_x} (\hat{\boldsymbol{J}}_{\boldsymbol{i}} \times \hat{\boldsymbol{J}}_{\boldsymbol{j}})^y - D \sum_{\langle \boldsymbol{i},\boldsymbol{j}\rangle_y} (\hat{\boldsymbol{J}}_{\boldsymbol{i}} \times \hat{\boldsymbol{J}}_{\boldsymbol{j}})^x + K \sum_{\langle \boldsymbol{i},\boldsymbol{j}\rangle_x} \hat{J}^y_{\boldsymbol{i}} \hat{J}^y_{\boldsymbol{j}} + K \sum_{\langle \boldsymbol{i},\boldsymbol{j}\rangle_y} \hat{J}^x_{\boldsymbol{i}} \hat{J}^x_{\boldsymbol{j}}, \quad (6)$$

with

$$J_1 = \frac{4}{9}\frac{(t_{11}+t_{33})^2}{U} - \frac{16}{9}\frac{(t_{\rm odd})^2}{U} = J_0 - J_{\rm odd}, \quad (7)$$

$$J_2 = \frac{4}{9}\frac{(t'_{33})^2}{U}, \quad (8)$$

$$D = \frac{16}{9}\frac{t_{\rm odd}(t_{11}+t_{33})}{U}, \quad (9)$$

$$K = 2J_{\rm odd}, \quad (10)$$

$\sum_{\langle \boldsymbol{i},\boldsymbol{j}\rangle} = \sum_{\langle \boldsymbol{i},\boldsymbol{j}\rangle_x} + \sum_{\langle \boldsymbol{i},\boldsymbol{j}\rangle_y}$, the sum of the summations taken over the NN sites along the x and y directions, and $\sum_{\langle\langle \boldsymbol{i},\boldsymbol{j}\rangle\rangle}$, the summation taken over the next-NN sites. Here we have neglected the products of the hole-density operators such as $\sum_{\langle \boldsymbol{i},\boldsymbol{j}\rangle} \hat{n}_{\boldsymbol{i}}\hat{n}_{\boldsymbol{j}}$ because such terms become constants in the mean-field approximation. Note that the finite terms of the DM-type interaction in Eq. (6) differ from the rotation-induced DM-type interaction[27]. In Sec. IV, we will discuss the effect of the $J_{\rm eff} = \frac{3}{2}$ states on the superexchange interactions.

The derived effective Hamiltonian Eq. (6) shows three effects of the IS breaking. One is to cause the DM-type interactions, $D\sum_{\langle \boldsymbol{i},\boldsymbol{j}\rangle_x}(\hat{\boldsymbol{J}}_{\boldsymbol{i}} \times \hat{\boldsymbol{J}}_{\boldsymbol{j}})^y$ and $-D\sum_{\langle \boldsymbol{i},\boldsymbol{j}\rangle_y}(\hat{\boldsymbol{J}}_{\boldsymbol{i}} \times \hat{\boldsymbol{J}}_{\boldsymbol{j}})^x$. Those interactions arise from the multiorbital superexchange interactions due to the combination of the even-mirror and the odd-mirror hopping integrals. Such combination is vital to obtain the DM-type antisymmetric interactions. This is because their operator parts behave like the functions odd about some coordinates in the symmetrical operations. For example, $(\hat{\boldsymbol{J}}_{\boldsymbol{i}} \times \hat{\boldsymbol{J}}_{\boldsymbol{j}})^x = \hat{J}^y_{\boldsymbol{i}}\hat{J}^z_{\boldsymbol{j}} - \hat{J}^z_{\boldsymbol{i}}\hat{J}^y_{\boldsymbol{j}}$ behaves like the function which is odd about y and z (and even about x); such function can be obtained by the multiorbital superexchange interactions using the even-mirror hopping integral and the odd-mirror hopping integral between the d_{xz} and the d_{xy} orbitals, which behaves like $xz \cdot xy = x^2y^1z^1$. Thus, the DM-type interactions originate from the mirror-mixing multiorbital effect. Another effect is to cause the ferromagnetic Heisenberg-type interaction, $-J_{\rm odd}\sum_{\langle \boldsymbol{i},\boldsymbol{j}\rangle} \hat{\boldsymbol{J}}_{\boldsymbol{i}} \cdot \hat{\boldsymbol{J}}_{\boldsymbol{j}}$. This interaction between the z components arises from a larger gain of the energy reduction due to the kinetic exchange between the same-J^z states than between the opposite-J^z states. This is because the number of processes in the former case is larger due to the opposite spin indices between the d_{xy} orbital and the d_{xz} or d_{yz} orbital in the $J^z = \pm\frac{1}{2}$ states[28]. Then, by including the pseudospin-flipping processes, we can obtain the ferromagnetic Heisenberg-type interaction because these processes give the $\hat{J}^+_{\boldsymbol{i}}\hat{J}^+_{\boldsymbol{j}}$ or $\hat{J}^-_{\boldsymbol{i}}\hat{J}^-_{\boldsymbol{j}}$ terms. The other effect is to cause the antiferromagentic Kitaev-type interactions, $K\sum_{\langle \boldsymbol{i},\boldsymbol{j}\rangle_x} \hat{J}^y_{\boldsymbol{i}}\hat{J}^y_{\boldsymbol{j}}$ and $K\sum_{\langle \boldsymbol{i},\boldsymbol{j}\rangle_y} \hat{J}^x_{\boldsymbol{i}}\hat{J}^x_{\boldsymbol{j}}$. This is because the above $J^+_{\boldsymbol{i}}J^+_{\boldsymbol{j}}$ or $\hat{J}^-_{\boldsymbol{i}}\hat{J}^-_{\boldsymbol{j}}$ terms give the extra $\hat{J}^x_{\boldsymbol{i}}\hat{J}^x_{\boldsymbol{j}}$ or $J^y_{\boldsymbol{i}}J^y_{\boldsymbol{j}}$ terms, and because the orbitals hybridized by $\hat{H}_{\rm odd}$ along the x and y direction have the finite off-diagonal matrix elements only of $\hat{L}^y_{\boldsymbol{i}}$ or $\hat{L}^x_{\boldsymbol{i}}$, respectively. Namely, the superexchange interactions between $\hat{L}^y_{\boldsymbol{i}}$ and $\hat{L}^y_{\boldsymbol{j}}$ along the x direction and between $\hat{L}^x_{\boldsymbol{i}}$ and $\hat{L}^x_{\boldsymbol{j}}$ along the y direction become antiferromagnetic in order to gain the energy reduction of the kinetic exchange due to the spin-independent interorbital hoppings of $\hat{H}_{\rm odd}$, resulting in the antiferromagnetic Kitaev-type interactions.

C. Mean-field approximation

For further understanding of the effects of the IS breaking, we analyze the ground state of Eq. (6) in the mean-field approximation. Since the energy in this approximation is quadratic about $\langle \hat{J}^\alpha_{\boldsymbol{q}}\rangle = \frac{1}{\sqrt{N}}\sum_{\boldsymbol{j}} e^{-i\boldsymbol{q}\cdot\boldsymbol{j}}\langle \hat{J}^\alpha_{\boldsymbol{j}}\rangle$, i.e.

$$\langle \hat{H}_{\rm eff}\rangle = \sum_{\boldsymbol{q}} \sum_{\alpha,\beta=x,y,z} J_{\alpha\beta}(\boldsymbol{q}) \langle \hat{J}^\alpha_{\boldsymbol{q}}\rangle^* \langle \hat{J}^\beta_{\boldsymbol{q}}\rangle, \quad (11)$$

we can determine the ground state by finding $\boldsymbol{q}$ of the lowest eigenvalue and the eigenvector of Eq. (11) with the periodic boundary condition and the constraints of the hard-pseudospin approximation,

$$\frac{1}{4} = \frac{1}{N}\sum_{\alpha}\sum_{\boldsymbol{q},\boldsymbol{q}'} e^{i(\boldsymbol{q}'-\boldsymbol{q})\cdot\boldsymbol{j}} \langle \hat{J}^\alpha_{\boldsymbol{q}}\rangle^* \langle \hat{J}^\alpha_{\boldsymbol{q}'}\rangle, \quad (12)$$

in which $\langle \hat{J}^\alpha_{\boldsymbol{i}}\rangle$ for all N sites are treated as the hard pseudospins for $J_{\rm eff} = \frac{1}{2}$. In Eq. (11), $J_{\alpha\beta}(\boldsymbol{q})$ are given

by

$$J_{xx}(\boldsymbol{q}) =(J_0 - J_{\rm odd})\cos q_x + (J_0 + J_{\rm odd})\cos q_y + 4J_2 \cos q_x \cos q_y, \quad (13)$$

$$J_{yy}(\boldsymbol{q}) =(J_0 + J_{\rm odd})\cos q_x + (J_0 - J_{\rm odd})\cos q_y + 4J_2 \cos q_x \cos q_y, \quad (14)$$

$$J_{zz}(\boldsymbol{q}) =(J_0 - J_{\rm odd})\cos q_x + (J_0 - J_{\rm odd})\cos q_y + 4J_2 \cos q_x \cos q_y, \quad (15)$$

$$J_{zx}(\boldsymbol{q}) = iD\sin q_x, \quad (16)$$

$$J_{xz}(\boldsymbol{q}) = -iD\sin q_x, \quad (17)$$

$$J_{zy}(\boldsymbol{q}) = iD\sin q_y, \quad (18)$$

$$J_{yz}(\boldsymbol{q}) = -iD\sin q_y. \quad (19)$$

The derivation of Eq. (11) from Eq. (6) is described in Appendix B.

III. RESULTS

Before the analyses with the IS breaking, we briefly explain the ground state without the IS breaking. Without it, the ground state is determined by the J_0 term and the J_2 term of Eq. (6). Namely, the ground state is a (π,π)-antiferromagnetic state for $J_0 > 4J_2$, and a $(\pi,0)$- or $(0,\pi)$-antiferromagnetic state for $J_0 < 4J_2$. The former is realized in a realistic case because $J_0 > 4J_2$ is satisfied due to $|t_{11}| \sim |t_{33}|$ and $|t'_{33}| < |t_{33}|$[29].

A. Stability of the screw states

To understand how the IS breaking affects the (π,π)-antiferromagnetic state, realized without the IS breaking, let us consider a minimal model with only the J_0 term and the D terms of Eq. (6). This minimal model is reasonable to analyze the essential effects of the IS breaking because D is larger than K for $2|t_{\rm odd}| < |t_{11} + t_{33}|$, corresponding to the case with the small effects of the IS breaking. (Such small-effect case is considered because the small effects are realized as long as the IS is broken.) For this minimal model, the lowest eigenvalue of Eq. (11) for each $\boldsymbol{q}$ is determined by

$$\lambda(\boldsymbol{q}) = J_0(\cos q_x + \cos q_y) - |D|\sqrt{(\sin q_x)^2 + (\sin q_y)^2}, \quad (20)$$

and it has three kinds of local minimum: (i) the (π,π)-antiferromagnetic state,

$$\lambda(\boldsymbol{Q}_{\rm AF}) = -2J_0 \quad (21)$$

with $\boldsymbol{Q}_{\rm AF} = (\pi,\pi)$; (ii) the one-directional-screw state,

$$\lambda(\boldsymbol{Q}_1) = -J_0 - \sqrt{J_0^2 + D^2} \quad (22)$$

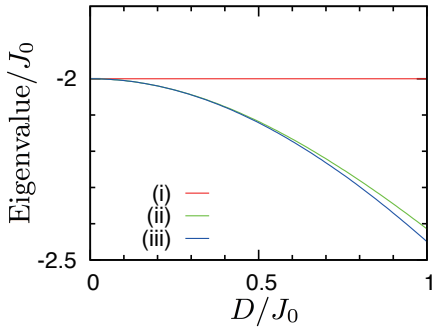

FIG. 2: (D/J_0) dependences of the eigenvalues divided by J_0 for states (i), (ii), and (iii) in the mean-field approximation for the minimal model.

with $\boldsymbol{Q}_1 = (\pm Q_1, \pi)$ or $\boldsymbol{Q}_1 = (\pi, \pm Q_1)$ for $Q_1 = \pi - \cos^{-1}(J_0/\sqrt{J_0^2 + D^2})$; and (iii) the two-directional-screw state,

$$\lambda(\boldsymbol{Q}_2) = -\sqrt{2}\sqrt{2J_0^2 + D^2} \quad (23)$$

with $\boldsymbol{Q}_2 = (\pm Q_2, \pm Q_2)$ or $\boldsymbol{Q}_2 = (\pm Q_2, \mp Q_2)$ for $Q_2 = \pi - \cos^{-1}(\sqrt{2}J_0/\sqrt{2J_0^2 + D^2})$.

In contrast to the (π,π)-antiferromagnetic state, those screw states show two unusual features. One is the spatial-dependent mixing between or among the components of $\langle \hat{J}_{\boldsymbol{i}}^{\alpha} \rangle$: for example, in the one-directional-screw state for $\boldsymbol{Q}_1 = (\pm Q_1, \pi)$,

$$\langle \hat{\boldsymbol{J}}_{\boldsymbol{i}} \rangle = \frac{1}{2}\begin{pmatrix} (-1)^{i_y+1}\mathrm{sgn}(D)\sin Q_1 i_x \\ 0 \\ (-1)^{i_y}\cos Q_1 i_x \end{pmatrix}; \quad (24)$$

and in the two-directional-screw state for $\boldsymbol{Q}_2 = (\pm Q_2, \pm Q_2)$,

$$\langle \hat{\boldsymbol{J}}_{\boldsymbol{i}} \rangle = \frac{1}{2}\begin{pmatrix} -\frac{1}{\sqrt{2}}\mathrm{sgn}(D)\sin \boldsymbol{Q}_2 \cdot \boldsymbol{i} \\ -\frac{1}{\sqrt{2}}\mathrm{sgn}(D)\sin \boldsymbol{Q}_2 \cdot \boldsymbol{i} \\ \cos \boldsymbol{Q}_2 \cdot \boldsymbol{i} \end{pmatrix}. \quad (25)$$

Thus, those screw states have the spatial variation of not only the spin distribution but also the orbital distribution because the spin and the orbital are highly entangled in the $J_{\rm eff} = \frac{1}{2}$ states[28] [see Eqs. (A1) and (A2)]. The other is the finite vector chirality: for example, in the one-directional-screw state for $\boldsymbol{Q}_1 = (\pm Q_1, \pi)$, the finite term is

$$\langle (\hat{\boldsymbol{J}}_{\boldsymbol{i}} \times \hat{\boldsymbol{J}}_{\boldsymbol{j}})^y \rangle = \frac{1}{4}(-1)^{i_y+j_y}\mathrm{sgn}(D)\sin Q_1 (j_x - i_x); \quad (26)$$

and in the two-directional-screw state for $\boldsymbol{Q}_2 = (\pm Q_2, \pm Q_2)$, the finite terms are

$$\langle (\hat{\boldsymbol{J}}_{\boldsymbol{i}} \times \hat{\boldsymbol{J}}_{\boldsymbol{j}})^x \rangle = \frac{1}{4\sqrt{2}}\mathrm{sgn}(D)\sin \boldsymbol{Q}_2 \cdot (\boldsymbol{j} - \boldsymbol{i}) \quad (27)$$

and

$$\langle (\hat{\boldsymbol{J}}_{\boldsymbol{i}} \times \hat{\boldsymbol{J}}_{\boldsymbol{j}})^y \rangle = -\frac{1}{4\sqrt{2}}\mathrm{sgn}(D)\sin \boldsymbol{Q}_2 \cdot (\boldsymbol{j} - \boldsymbol{i}). \quad (28)$$

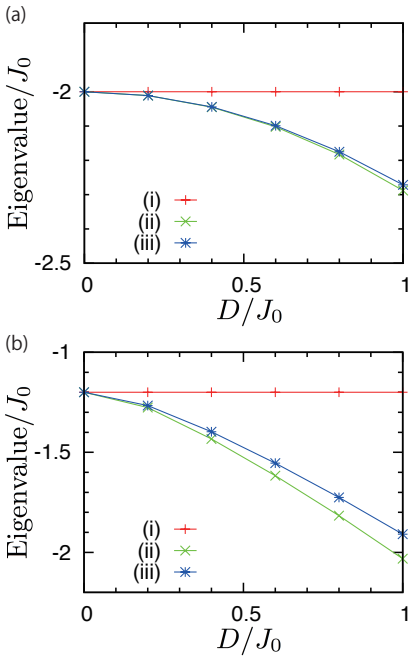

FIG. 3: (D/J_0) dependences of the eigenvalues divided by J_0 for states (i), (ii), and (iii) in the mean-field approximation with $N = 100 \times 100$ meshes for the model with the J_0 and the D terms, $J_{\rm odd} = \frac{1}{4}J_0(\frac{D}{J_0})^2$, and $J_2 =$ (a) 0 or (b) $0.2J_0$.

Thus, those screw states have the spin-orbital-coupled vector chirality.

From the (D/J_0) dependences of the eigenvalues of states (i), (ii), and (iii), shown in Fig. 2, we find that the screw states are more stable than the (π, π)-antiferromagnetic state, and that the most stable state in the minimal model is the two-directional-screw state. The stabilities of those screw states can be understood that the J_0 term becomes minimum for $\boldsymbol{q} = (\pi, \pi)$, and the D terms become minimum for $\boldsymbol{q} = (\frac{\pi}{2}, \frac{\pi}{2})$.

B. Limit of the hard-pseudospin approximation

Even in the presence of the J_2 term and the $J_{\rm odd}$ terms, the eigenvalues of the screw states are lower than the eigenvalue for $\boldsymbol{q} = (\pi, \pi)$, as shown in Figs. 3(a) and 3(b). In particular, the one-directional-screw state for $\boldsymbol{Q}'_1 = (\pm Q'_1, \pi)$ or $\boldsymbol{q} = (\pi, \pm Q'_1)$ gives the lowest eigenvalue (see those figures). This is because the $J_{\rm odd}$ terms and the J_2 term destabilize the states for $\boldsymbol{q} = (Q, \pm Q)$. Namely, the lowest eigenvalue of the one-directional-screw state arises from the combination of the stabilization of the screw states due to the D terms and the destabilization of the two-directional-screw state (compared with the one-directional-screw state) due to the $J_{\rm odd}$ terms and the J_2 term.

In contrast to the case of the minimal model, the screw states in the presence of the $J_{\rm odd}$ terms do not satisfy the hard-pseudospin constraints of $\langle \hat{\boldsymbol{J}}_{\boldsymbol{j}} \rangle$. This is because under the constraints, the possible one-directional-screw state is restricted to $\langle \hat{\boldsymbol{J}}_{\boldsymbol{Q}} \rangle = {}^t(\pm ib, 0, b)$ or $\langle \hat{\boldsymbol{J}}_{\boldsymbol{Q}} \rangle = {}^t(0, \pm ib, b)$, although in the presence of the anisotropic terms such as the $J_{\rm odd}$ terms the realized state becomes $\langle \hat{\boldsymbol{J}}_{\boldsymbol{Q}} \rangle = {}^t(\pm ib, 0, c)$ or $\langle \hat{\boldsymbol{J}}_{\boldsymbol{Q}} \rangle = {}^t(0, \pm ib, c)$ with $c \neq b$. The situation is similar even for the two-directional-screw state. This problem exists even for a small value of $J_{\rm odd}$, for which the $J_{\rm odd}$ terms act as the weak perturbation against the J_0 term and the D terms. Such weak perturbation will not break the stability of the one-directional-screw state at least in a non-frustrated system. Thus, this result highlights the limit of the hard-pseudospin approximation in discussing the stability of the screw states in the presence of the anisotropic exchange interactions. Namely, for such discussions, we need to take into account the quantum fluctuations, which cause softness of the pseudospins. Further details about the meanings of this result are discussed in Sec. IV. Since this work is the first step towards a satisfactory understanding of the spin-orbital-coupled chirality in a non-frustrated Mott insulator with the strong SOC, the analysis including the quantum fluctuations is a future work.

IV. DISCUSSION

I first discuss the meanings of the limit of the hard-pseudospin approximation in detail. The key to the limit is a conflict between the states stabilized by the DM-type and the Kitaev-type interactions. The DM-type interactions stabilize the states in which some components of $\langle \hat{J}^{\alpha}_{\boldsymbol{Q}} \rangle$ (e.g., $\langle \hat{J}^{x}_{\boldsymbol{Q}} \rangle$ and $\langle \hat{J}^{z}_{\boldsymbol{Q}} \rangle$) are mixed under a certain condition (e.g., $|\langle \hat{J}^{x}_{\boldsymbol{Q}} \rangle| = |\langle \hat{J}^{z}_{\boldsymbol{Q}} \rangle|$). On the other hand, the Kitaev-type interactions stabilize the states in which one component is different from the others (e.g., for the Kitaev-type interactions of the z component, $|\langle \hat{J}^{z}_{\boldsymbol{Q}} \rangle| \neq |\langle \hat{J}^{x}_{\boldsymbol{Q}} \rangle|, |\langle \hat{J}^{y}_{\boldsymbol{Q}} \rangle|$). Thus, the states stabilized by the DM-type and the Kitaev-type interactions are generally incompatible within the hard-pseudospin approximation. This property may hold in other systems with the strong SOC, where the DM-type and the Kitaev-type interactions appear. Then, this property has difficulty in calculating the pseudospin-wave dispersions because the pseudospin-wave dispersions are usually calculated by considering the quantum fluctuations around the most stable state in the hard pseudospin approximation. Since the hard-pseudospin approximation is used in not only the mean-field approximation but also the Luttinger-Tisza method[30] and the classical Monte Carlo calculation, which are frequently used in the theoretical studies for systems with the strong SOC, the result of the limit of the hard-pseudospin approximation provides an important step for research of the systems with the strong SOC.

Then, we discuss the effects of the tetragonal crystal field and the $J_{\rm eff} = \frac{3}{2}$ states. As we will see below, the treatment of those in this paper is appropriate for qualitative analyses. In particular, the treatment is sufficient

to clarify the main issue, i.e., whether not only the spin but also the orbital acquires the chirality for the strong SOC in the situation in which the spin acquires the chirality for the weak SOC.

We begin with the effect of the tetragonal crystal field, $\Delta_{\rm tetra}$. Since we consider a 214-type perovskite oxide, such as Sr_2IrO_4, $\Delta_{\rm tetra}$ becomes finite; $\Delta_{\rm tetra}$ splits the t_{2g} orbitals into the d_{xy} orbital and the degenerate d_{xz} and d_{yz} orbitals. To show the validity of neglecting its effect for qualitative analyses, let us consider two limiting cases, (i) $\lambda_{LS} \ll \Delta_{\rm tetra}$ and (ii) $\lambda_{LS} \gg \Delta_{\rm tetra}$; the limiting cases are sufficient for qualitative analyses, while the nonlimiting cases are necessary for quantitative analyses. Case (i) is inappropriate to analyze the magnetic properties in the presence of the formation of the spin-orbital-coupled degree of freedom because the ground state in case (i) is the state that one hole occupies either the d_{xy} orbital or the degenerate d_{xz} and d_{yz} orbitals, depending on the sign of $\Delta_{\rm tetra}$. On the other hand, in case (ii), we can analyze the effect of $\Delta_{\rm tetra}$ on the magnetic properties for the $J_{\rm eff}$ states. Since we consider $\lambda_{LS} \gg \Delta_{\rm tetra}$ in $U, U' \gg \lambda_{LS} \gg |t^{\rm (even)}_{ab;\boldsymbol{ij}}|, |t^{\rm (odd)}_{ab;\boldsymbol{ij}}|$, the effect of $\Delta_{\rm tetra}$ is negligible compared with the effect of U.

We turn to the effect of the $J_{\rm eff} = \frac{3}{2}$ states. Due to the non-perturbative treatment of the SOC, the t_{2g} orbitals are split into the $J_{\rm eff} = \frac{1}{2}$ states and the $J_{\rm eff} = \frac{3}{2}$ states. In the ground state for the $(t_{2g})^5$-electron configuration, four electrons per site occupy the $J_{\rm eff} = \frac{3}{2}$ states and one electron per site occupies the $J_{\rm eff} = \frac{1}{2}$ states; this is equivalent to the configuration in which one hole per site occupies the $J_{\rm eff} = \frac{1}{2}$ states. In this configuration, the $J_{\rm eff} = \frac{3}{2}$ states do not affect the initial and final states of the perturbation calculations for the ground state because the initial and final states are the lowest-energy states for the non-perturbative Hamiltonian. On the other hand, the $J_{\rm eff} = \frac{3}{2}$ states affect the intermediate states of the perturbation calculations. This effect is taken into account in our calculations. This is because we consider $U \gg \lambda_{LS}$, in which the intermediate states are approximately given by the two-hole's eigenstates for $\hat{H}_{\rm int}$ [see Eq. (A24)], and because those eigenstates include two-hole's states not only for the $J_{\rm eff} = \frac{1}{2}$ states but also for the $J_{\rm eff} = \frac{3}{2}$ states. The above treatment of the $J_{\rm eff} = \frac{3}{2}$ states is sufficient for qualitative analyses of the magnetic properties, while for the quantitative analysis, we may consider the superexchange interactions derived in the second-lowest-energy states in which three electrons occupy the $J_{\rm eff} = \frac{3}{2}$ states and two electrons occupy the $J_{\rm eff} = \frac{1}{2}$ states.

Finally, let us apply the present theory to the quasi-two-dimensional insulating iridates near the [001]-surface of Sr_2IrO_4 and the interface between Sr_2IrO_4 and $Sr_3Ir_2O_7$. First, the effects of the IS breaking near the surface and the interface are described by $\hat{H}_{\rm odd}$ because $\hat{H}_{\rm odd}$ can describe the effects of ab-plane's IS breaking on the quasi-two-dimensional t_{2g}-orbital systems (e.g., the Ru oxides[22,23] and Ti oxides[31]). In addition, the (π,π) antiferromagnetism[32,33] in Sr_2IrO_4 can be understood within the mean-field approximation for the superexchange interactions derived from $\hat{H}$ for $t_{\rm odd} = 0$. Although the (π,π)-antiferromagnetic state becomes most stable for the realistic parameters, $J_{\rm H} > 0$ and $|t_{11}| > |t_{33}|$ are necessary to understand the difference between the in-plane and the out-of-plane alignments of the (π,π)-antiferromagnetic moments. This is because the main terms stabilizing the in-plane and the out-of-plane alignments for $t_{\rm odd} = 0$ are $\frac{8}{9}\frac{(t_{11})^2 J_{\rm H}}{(U')^2+(J_{\rm H})^2}[\sum_{\langle \boldsymbol{i},\boldsymbol{j}\rangle_x} \hat{J}^y_{\boldsymbol{i}}\hat{J}^y_{\boldsymbol{j}} + \sum_{\langle \boldsymbol{i},\boldsymbol{j}\rangle_y} \hat{J}^x_{\boldsymbol{i}}\hat{J}^x_{\boldsymbol{j}}] + \frac{16}{9}\frac{t_{11}t_{33}J_{\rm H}}{(U')^2+(J_{\rm H})^2}[\sum_{\langle \boldsymbol{i},\boldsymbol{j}\rangle_x} \hat{J}^x_{\boldsymbol{i}}\hat{J}^x_{\boldsymbol{j}} + \sum_{\langle \boldsymbol{i},\boldsymbol{j}\rangle_y} \hat{J}^y_{\boldsymbol{i}}\hat{J}^y_{\boldsymbol{j}}]$ and $\frac{8}{9}\frac{(t_{33})^2 J_{\rm H}}{(U')^2+(J_{\rm H})^2}\sum_{\langle \boldsymbol{i},\boldsymbol{j}\rangle} \hat{J}^z_{\boldsymbol{i}}\hat{J}^z_{\boldsymbol{j}}$, respectively [see Eqs. (A25) and (A27)], and because the former terms are dominant for $|t_{11}| > |t_{33}|$. However, even in the presence of the anisotropies for $J_{\rm H} > 0$, the screw states may be more stable than the (π,π)-antiferromagnetic state by introducing ab-plane's IS breaking if the Heisenberg-type interactions between the z components remain finite. This is because the finite Heisenberg-type interactions between the z components and the x/y components are necessary to stabilize the screw states by using the DM-type interactions due to ab-plane's IS breaking. Then, the effects of the rotation[34] of IrO_6 octahedra for the small angle ($\simeq 11^\circ$) will not qualitatively change the emergence of the spin-orbital-coupled vector chirality. This is because its most drastic effect is to induce the small canted angle of the in-plane aligned moments of Sr_2IrO_4[27], and because the coefficient of the D terms is made to be larger than the coefficients of the rotation-induced exchange interactions[27] (which are small for the small angle) by tuning the value of $t_{\rm odd}$ with keeping the rotation angle small. Thus, the candidates for the spin-orbital-coupled vector chirality are the quasi-two-dimensional insulating iridates near the [001]-surface of Sr_2IrO_4 and the interface between Sr_2IrO_4 and $Sr_3Ir_2O_7$.

V. SUMMARY

In summary, I have studied the effects of the IS broken near an ab plane of a quasi-two-dimensional insulating iridate using the low-energy effective Hamiltonian of the superexchange interactions. I find that the DM-type interactions, induced by the IS breaking, cause the spin-orbital-coupled vector chirality as a result of stabilizing the screw state compared with the (π,π)-antiferromagnetic state. I also find that in the presence of both the DM-type and the Kitaev-type interactions, the hard-pseudospin approximation becomes inappropriate to analyze the stability of the screw state. Then, I discuss the effects of the tetragonal crystal field and the $J_{\rm eff} = \frac{3}{2}$ states, and show the validity of their treatment for qualitative analyses. I finally argue that the candidates for realizing the spin-orbital-coupled vector chirality are the iridates near the [001] surface of Sr_2IrO_4 and

the interface between Sr_2IrO_4 and $Sr_3Ir_2O_7$. The finding of the spin-orbital-coupled vector chirality provides a new possibility of utilizing the chirality of the anisotropic spatial distribution of electrons/holes in a non-frustrated Mott insulator with the strong SOC by introducing the IS breaking.

Acknowledgments

The author thanks T. Mizoguchi for useful comments about the previous theoretical studies in the frustrated iridates. For the numerical calculations, the author used the facilities of the Super Computer Center, the Institute for Solid State Physics, the University of Tokyo.

Appendix A: Derivation of Eq. (6)

In this appendix, I derive Eq. (6) by calculating the superexchange interactions in the Mott insulator for $\hat{H}$. This derivation is the extension of the formulation[26] for a t_{2g}-orbital Hubbard model without the SOC to the case with the SOC. The treatment of the SOC is similar to that for Refs. 15 and 17.

In this derivation, we use three assumptions, resulting in the condition $U, U' \gg \lambda_{LS} \gg |t^{(\mathrm{even})}_{ab;\boldsymbol{ij}}|, |t^{(\mathrm{odd})}_{ab;\boldsymbol{ij}}|$. We first assume that the hopping integrals of $\hat{H}_{\mathrm{even}}$ and $\hat{H}_{\mathrm{odd}}$, $t^{(\mathrm{even})}_{ab;\boldsymbol{ij}}$ and $t^{(\mathrm{odd})}_{ab;\boldsymbol{ij}}$, are smaller than U and U'. Thus, we can treat the effects of $\hat{H}_{\mathrm{even}}$ and $\hat{H}_{\mathrm{odd}}$ as the second-order perturbation against the interaction terms. Also, we assume that the SOC, λ_{LS}, is larger than $|t^{(\mathrm{even})}_{ab;\boldsymbol{ij}}|$ and $|t^{(\mathrm{odd})}_{ab;\boldsymbol{ij}}|$; as a result, the excitations from the $J_{\mathrm{eff}} = \frac{1}{2}$ states to the $J_{\mathrm{eff}} = \frac{3}{2}$ states are negligible. Thus, the nonperturbed states of two sites ($\boldsymbol{i} = \mathbf{1}, \mathbf{2}$) are given by the products of the $J^z = \pm\frac{1}{2}$ states[28], i.e. $|+,+\rangle = |\mathbf{1},+\rangle|\mathbf{2},+\rangle$, $|+,-\rangle = |\mathbf{1},+\rangle|\mathbf{2},-\rangle$, $|-,+\rangle = |\mathbf{1},-\rangle|\mathbf{2},+\rangle$, and $|-,-\rangle = |\mathbf{1},-\rangle|\mathbf{2},-\rangle$ with

$$|\boldsymbol{i},+\rangle = \frac{1}{\sqrt{3}}(i\hat{c}^{\dagger}_{\boldsymbol{i}d_{xz}\downarrow} + \hat{c}^{\dagger}_{\boldsymbol{i}d_{yz}\downarrow} + \hat{c}^{\dagger}_{\boldsymbol{i}d_{xy}\uparrow})|0\rangle, \tag{A1}$$

$$|\boldsymbol{i},-\rangle = \frac{1}{\sqrt{3}}(i\hat{c}^{\dagger}_{\boldsymbol{i}d_{xz}\uparrow} - \hat{c}^{\dagger}_{\boldsymbol{i}d_{yz}\uparrow} + \hat{c}^{\dagger}_{\boldsymbol{i}d_{xy}\downarrow})|0\rangle. \tag{A2}$$

Moreover, for simplicity of the formulation, we assume that λ_{LS} is smaller than U and U'. Because of this assumption, we can neglect the effects of λ_{LS} on the energy of the intermediate states of the second-order perturbation, i.e. $\frac{1}{E_0 - \hat{H}_{\mathrm{int}} - \hat{H}_{LS}} \sim \frac{1}{-\hat{H}_{\mathrm{int}}}$. Note that since $\hat{H}_{\mathrm{int}}$ is rewritten in terms of the irreducible representations for the two-hole states per site [see Eq. (A4)], the condition $U, U' \gg \lambda_{LS}$ implies that the energies of all the irreducible representations, which include either U or U', are larger than λ_{LS}, i.e. $U_\Gamma \gg \lambda_{LS}$.

Under the condition $U, U' \gg \lambda_{LS} \gg |t^{(\mathrm{even})}_{ab;\boldsymbol{ij}}|, |t^{(\mathrm{odd})}_{ab;\boldsymbol{ij}}|$, we derive the Hamiltonian of the superexchange interactions between the two neighboring sites, $(\hat{H}_{\mathrm{eff}})_{\mathbf{12}}$, from

$$(\hat{H}_{\mathrm{eff}})_{\mathbf{12}} = \langle f|(\hat{H}_{\mathrm{even}} + \hat{H}_{\mathrm{odd}})\frac{1}{-\hat{H}_{\mathrm{int}}}(\hat{H}_{\mathrm{even}} + \hat{H}_{\mathrm{odd}})|i\rangle \times |f\rangle\langle i|, \tag{A3}$$

with $\{|i\rangle, |f\rangle\} = \{|+,+\rangle, |+,-\rangle, |-,+\rangle, |-,-\rangle\}$. For example, for $|i\rangle = |+,+\rangle$ and $|f\rangle = |+,+\rangle$, $|f\rangle\langle i|$ is given by the operator $(\frac{1}{2}\hat{n}_{\mathbf{1}} - \hat{J}^z_{\mathbf{1}})(\frac{1}{2}\hat{n}_{\mathbf{2}} - \hat{J}^z_{\mathbf{2}})$; for $|i\rangle = |+,-\rangle$ and $|f\rangle = |-,+\rangle$, $|f\rangle\langle i|$ is given by the operator $\hat{J}^-_{\mathbf{1}}\hat{J}^+_{\mathbf{2}}$.

For easy treatment of $\hat{H}_{\mathrm{int}}$ in Eq. (A3), we rewrite $\hat{H}_{\mathrm{int}}$ in terms of the irreducible representations[26] for the two-hole states, the intermediate states in the second-order perturbation:

$$\hat{H}_{\mathrm{int}} = \sum_{\boldsymbol{i}}\sum_{\Gamma}\sum_{g_\Gamma} U_\Gamma |\boldsymbol{i};\Gamma,g_\Gamma\rangle\langle\boldsymbol{i};\Gamma,g_\Gamma|, \tag{A4}$$

where Γ denotes the irreducible representations, and g_Γ denotes the degeneracy. For the two-hole states of the t_{2g}-orbital Hubbard model, there are four kinds of U_Γ:

$$U_{A_1} = U + 2J', \tag{A5}$$

$$U_E = U - J', \tag{A6}$$

$$U_{T_1} = U' - J_{\mathrm{H}}, \tag{A7}$$

$$U_{T_2} = U' + J_{\mathrm{H}}; \tag{A8}$$

and $|\boldsymbol{i};\Gamma,g_\Gamma\rangle$ are

$$|\boldsymbol{i};A_1\rangle = \frac{1}{\sqrt{3}}(\hat{c}^\dagger_{\boldsymbol{i}d_{xz}\uparrow}\hat{c}^\dagger_{\boldsymbol{i}d_{xz}\downarrow} + \hat{c}^\dagger_{\boldsymbol{i}d_{yz}\uparrow}\hat{c}^\dagger_{\boldsymbol{i}d_{yz}\downarrow} + \hat{c}^\dagger_{\boldsymbol{i}d_{xy}\uparrow}\hat{c}^\dagger_{\boldsymbol{i}d_{xy}\downarrow})|0\rangle, \tag{A9}$$

$$|\boldsymbol{i};E,u\rangle = \sqrt{\frac{2}{3}}(-\hat{c}^\dagger_{\boldsymbol{i}d_{xz}\uparrow}\hat{c}^\dagger_{\boldsymbol{i}d_{xz}\downarrow} + \frac{1}{2}\hat{c}^\dagger_{\boldsymbol{i}d_{yz}\uparrow}\hat{c}^\dagger_{\boldsymbol{i}d_{yz}\downarrow} + \frac{1}{2}\hat{c}^\dagger_{\boldsymbol{i}d_{xy}\uparrow}\hat{c}^\dagger_{\boldsymbol{i}d_{xy}\downarrow})|0\rangle, \tag{A10}$$

$$|\boldsymbol{i};E,v\rangle = \frac{1}{\sqrt{2}}(\hat{c}^\dagger_{\boldsymbol{i}d_{yz}\uparrow}\hat{c}^\dagger_{\boldsymbol{i}d_{yz}\downarrow} - \hat{c}^\dagger_{\boldsymbol{i}d_{xy}\uparrow}\hat{c}^\dagger_{\boldsymbol{i}d_{xy}\downarrow})|0\rangle, \tag{A11}$$

$$|\boldsymbol{i};T_1,\zeta_+\rangle = \hat{c}^\dagger_{\boldsymbol{i}d_{xz}\uparrow}\hat{c}^\dagger_{\boldsymbol{i}d_{yz}\uparrow}|0\rangle, \tag{A12}$$

$$|\boldsymbol{i};T_1,\zeta_-\rangle = \hat{c}^\dagger_{\boldsymbol{i}d_{xz}\downarrow}\hat{c}^\dagger_{\boldsymbol{i}d_{yz}\downarrow}|0\rangle, \tag{A13}$$

$$|\boldsymbol{i};T_1,\zeta_0\rangle = \frac{1}{\sqrt{2}}(\hat{c}^\dagger_{\boldsymbol{i}d_{xz}\uparrow}\hat{c}^\dagger_{\boldsymbol{i}d_{yz}\downarrow} + \hat{c}^\dagger_{\boldsymbol{i}d_{xz}\downarrow}\hat{c}^\dagger_{\boldsymbol{i}d_{yz}\uparrow})|0\rangle, \tag{A14}$$

$$|\boldsymbol{i};T_2,\zeta_0\rangle = \frac{1}{\sqrt{2}}(\hat{c}^\dagger_{\boldsymbol{i}d_{xz}\uparrow}\hat{c}^\dagger_{\boldsymbol{i}d_{yz}\downarrow} - \hat{c}^\dagger_{\boldsymbol{i}d_{xz}\downarrow}\hat{c}^\dagger_{\boldsymbol{i}d_{yz}\uparrow})|0\rangle, \tag{A15}$$

$$|\boldsymbol{i};T_1,\xi_+\rangle = \hat{c}^\dagger_{\boldsymbol{i}d_{xz}\uparrow}\hat{c}^\dagger_{\boldsymbol{i}d_{xy}\uparrow}|0\rangle, \tag{A16}$$

$$|\boldsymbol{i};T_1,\xi_-\rangle = \hat{c}^\dagger_{\boldsymbol{i}d_{xz}\downarrow}\hat{c}^\dagger_{\boldsymbol{i}d_{xy}\downarrow}|0\rangle, \tag{A17}$$

$$|\boldsymbol{i};T_1,\xi_0\rangle = \frac{1}{\sqrt{2}}(\hat{c}^\dagger_{\boldsymbol{i}d_{xz}\uparrow}\hat{c}^\dagger_{\boldsymbol{i}d_{xy}\downarrow} + \hat{c}^\dagger_{\boldsymbol{i}d_{xz}\downarrow}\hat{c}^\dagger_{\boldsymbol{i}d_{xy}\uparrow})|0\rangle, \tag{A18}$$

$$|\boldsymbol{i};T_2,\xi_0\rangle = \frac{1}{\sqrt{2}}(\hat{c}^\dagger_{\boldsymbol{i}d_{xz}\uparrow}\hat{c}^\dagger_{\boldsymbol{i}d_{xy}\downarrow} - \hat{c}^\dagger_{\boldsymbol{i}d_{xz}\downarrow}\hat{c}^\dagger_{\boldsymbol{i}d_{xy}\uparrow})|0\rangle, \tag{A19}$$

$$|\boldsymbol{i};T_1,\eta_+\rangle = \hat{c}^\dagger_{\boldsymbol{i}d_{yz}\uparrow}\hat{c}^\dagger_{\boldsymbol{i}d_{xy}\uparrow}|0\rangle, \tag{A20}$$

$$|\boldsymbol{i};T_1,\eta_-\rangle = \hat{c}^\dagger_{\boldsymbol{i}d_{yz}\downarrow}\hat{c}^\dagger_{\boldsymbol{i}d_{xy}\downarrow}|0\rangle, \tag{A21}$$

$$|\boldsymbol{i};T_1,\eta_0\rangle = \frac{1}{\sqrt{2}}(\hat{c}^\dagger_{\boldsymbol{i}d_{yz}\uparrow}\hat{c}^\dagger_{\boldsymbol{i}d_{xy}\downarrow} + \hat{c}^\dagger_{\boldsymbol{i}d_{yz}\downarrow}\hat{c}^\dagger_{\boldsymbol{i}d_{xy}\uparrow})|0\rangle, \tag{A22}$$

$$|\boldsymbol{i};T_2,\eta_0\rangle = \frac{1}{\sqrt{2}}(\hat{c}^\dagger_{\boldsymbol{i}d_{yz}\uparrow}\hat{c}^\dagger_{\boldsymbol{i}d_{xy}\downarrow} - \hat{c}^\dagger_{\boldsymbol{i}d_{yz}\downarrow}\hat{c}^\dagger_{\boldsymbol{i}d_{yx}\uparrow})|0\rangle. \tag{A23}$$

By substituting Eq. (A4) into Eq. (A3), Eq. (A3) becomes

$$(\hat{H}_{\rm eff})_{\mathbf{12}} = \sum_{\boldsymbol{i}=\mathbf{1},\mathbf{2}}\sum_{\Gamma}\sum_{g_\Gamma}\langle f|(\hat{H}_{\rm even}+\hat{H}_{\rm odd})|\boldsymbol{i};\Gamma,g_\Gamma\rangle \times \frac{1}{-U_\Gamma}\langle\boldsymbol{i};\Gamma,g_\Gamma|(\hat{H}_{\rm even}+\hat{H}_{\rm odd})|i\rangle|f\rangle\langle i|. \tag{A24}$$

Thus, the remaining tasks are to calculate the right-hand side of Eq. (A24) for $\mathbf{2}-\mathbf{1} = (1,0)$, $(0,1)$, $(1,1)$, and $(1,-1)$. Those components are sufficient to derive the superexchange interactions for $\hat{H}$ since all the components in the model considered are categorized into the terms along x, y, [110], and [1$\bar{1}$0] directions.

Let us first derive the terms of $(\hat{H}_{\rm eff})_{\mathbf{12}}$ for $\mathbf{2}-\mathbf{1} = (1,0)$. In this case, the finite terms of $(\hat{H}_{\rm even}+\hat{H}_{\rm odd})$ come from the finite hopping integrals along the x direction: for $\hat{H}_{\rm even}$, the hopping integral between the d_{xz} orbitals at **1** and **2**, $-t_{11}$, and the hopping integral between the d_{xy} orbitals, $-t_{33}$; for $\hat{H}_{\rm odd}$, the hopping integral between the d_{yz} orbital at **1** and the d_{xy} orbital at **2**, $-t_{\rm odd}$, and the hopping integral between the d_{xy} orbital at **1** and the d_{yz} orbital at **2**, $+t_{\rm odd}$. By applying one of those hopping terms to |i⟩, one of the four degenerate states (i.e., $|+,+\rangle$, $|+,-\rangle$, $|-,+\rangle$, and $|-,-\rangle$), and using Eqs. (A9)–(A23), we obtain the finite terms of $\langle\boldsymbol{i};\Gamma,g_\Gamma|(\hat{H}_{\rm even}+\hat{H}_{\rm odd})|i\rangle$ for $\boldsymbol{i}=\mathbf{1}$ or **2**. We similarly obtain the finite terms of $\langle f|(\hat{H}_{\rm even}+\hat{H}_{\rm odd})|\boldsymbol{i};\Gamma,g_\Gamma\rangle$ for $\boldsymbol{i}=\mathbf{1}$ or **2**. By combining those results with Eq. (A24), the superexchange interactions for $\mathbf{2}-\mathbf{1}=(1,0)$ are given by

$$\begin{aligned}
(\hat{H}_{\rm eff})_{\mathbf{12}} =& -\frac{4}{27}(\frac{t_{11}^2}{U+2J'}+\frac{2t_{11}^2}{U-J'})(\frac{1}{4}\hat{n}_{\mathbf{1}}\hat{n}_{\mathbf{2}}-\hat{\boldsymbol{J}}_{\mathbf{1}}\cdot\hat{\boldsymbol{J}}_{\mathbf{2}})\\
&-\frac{4}{9}\frac{t_{11}^2}{U'-J_{\rm H}}(\frac{3}{4}\hat{n}_{\mathbf{1}}\hat{n}_{\mathbf{2}}-\hat{J}^y_{\mathbf{1}}\hat{J}^y_{\mathbf{2}})-\frac{4}{9}\frac{t_{11}^2}{U'+J_{\rm H}}(\frac{1}{4}\hat{n}_{\mathbf{1}}\hat{n}_{\mathbf{2}}+\hat{J}^y_{\mathbf{1}}\hat{J}^y_{\mathbf{2}})\\
&-\frac{4}{27}(\frac{t_{33}^2}{U+2J'}+\frac{2t_{33}^2}{U-J'})(\frac{1}{4}\hat{n}_{\mathbf{1}}\hat{n}_{\mathbf{2}}-\hat{\boldsymbol{J}}_{\mathbf{1}}\cdot\hat{\boldsymbol{J}}_{\mathbf{2}})\\
&-\frac{4}{9}\frac{t_{33}^2}{U'-J_{\rm H}}(\frac{3}{4}\hat{n}_{\mathbf{1}}\hat{n}_{\mathbf{2}}-\hat{J}^z_{\mathbf{1}}\hat{J}^z_{\mathbf{2}})-\frac{4}{9}\frac{t_{33}^2}{U'+J_{\rm H}}(\frac{1}{4}\hat{n}_{\mathbf{1}}\hat{n}_{\mathbf{2}}+\hat{J}^z_{\mathbf{1}}\hat{J}^z_{\mathbf{2}})\\
&-\frac{8}{27}(\frac{t_{11}t_{33}}{U+2J'}-\frac{t_{11}t_{33}}{U-J'})(\frac{1}{4}\hat{n}_{\mathbf{1}}\hat{n}_{\mathbf{2}}-\hat{\boldsymbol{J}}_{\mathbf{1}}\cdot\hat{\boldsymbol{J}}_{\mathbf{2}})\\
&+\frac{4}{9}\frac{t_{11}t_{33}}{U'-J_{\rm H}}(\frac{1}{4}\hat{n}_{\mathbf{1}}\hat{n}_{\mathbf{2}}+\hat{\boldsymbol{J}}_{\mathbf{1}}\cdot\hat{\boldsymbol{J}}_{\mathbf{2}}+2\hat{J}^x_{\mathbf{1}}\hat{J}^x_{\mathbf{2}})\\
&+\frac{4}{9}\frac{t_{11}t_{33}}{U'+J_{\rm H}}(\frac{1}{4}\hat{n}_{\mathbf{1}}\hat{n}_{\mathbf{2}}+\hat{\boldsymbol{J}}_{\mathbf{1}}\cdot\hat{\boldsymbol{J}}_{\mathbf{2}}-2\hat{J}^x_{\mathbf{1}}\hat{J}^x_{\mathbf{2}})\\
&-\frac{8}{27}(\frac{2t_{\rm odd}^2}{U+2J'}+\frac{t_{\rm odd}^2}{U-J'})(\frac{1}{4}\hat{n}_{\mathbf{1}}\hat{n}_{\mathbf{2}}+\hat{\boldsymbol{J}}_{\mathbf{1}}\cdot\hat{\boldsymbol{J}}_{\mathbf{2}}-2\hat{J}^y_{\mathbf{1}}\hat{J}^y_{\mathbf{2}})\\
&-\frac{4}{9}\frac{t_{\rm odd}^2}{U'-J_{\rm H}}(\frac{5}{4}\hat{n}_{\mathbf{1}}\hat{n}_{\mathbf{2}}+2\hat{\boldsymbol{J}}_{\mathbf{1}}\cdot\hat{\boldsymbol{J}}_{\mathbf{2}}-5\hat{J}^y_{\mathbf{1}}\hat{J}^y_{\mathbf{2}})\\
&-\frac{4}{9}\frac{t_{\rm odd}^2}{U'+J_{\rm H}}(\frac{1}{4}\hat{n}_{\mathbf{1}}\hat{n}_{\mathbf{2}}+\hat{J}^y_{\mathbf{1}}\hat{J}^y_{\mathbf{2}})\\
&-\frac{16}{27}(\frac{t_{11}t_{\rm odd}}{U+2J'}-\frac{t_{11}t_{\rm odd}}{U-J'})(\hat{J}^x_{\mathbf{1}}\hat{J}^z_{\mathbf{2}}-\hat{J}^z_{\mathbf{1}}\hat{J}^x_{\mathbf{2}})\\
&-\frac{16}{9}\frac{t_{11}t_{\rm odd}}{U'-J_{\rm H}}(\hat{J}^x_{\mathbf{1}}\hat{J}^z_{\mathbf{2}}-\hat{J}^z_{\mathbf{1}}\hat{J}^x_{\mathbf{2}})\\
&-\frac{16}{27}(\frac{t_{33}t_{\rm odd}}{U+2J'}+\frac{1}{2}\frac{t_{33}t_{\rm odd}}{U-J'})(\hat{J}^x_{\mathbf{1}}\hat{J}^z_{\mathbf{2}}-\hat{J}^z_{\mathbf{1}}\hat{J}^x_{\mathbf{2}})\\
&-\frac{8}{9}\frac{t_{33}t_{\rm odd}}{U'-J_{\rm H}}(\hat{J}^x_{\mathbf{1}}\hat{J}^z_{\mathbf{2}}-\hat{J}^z_{\mathbf{1}}\hat{J}^x_{\mathbf{2}}).
\end{aligned}\tag{A25}$$

In the above derivation, we have used the relations, $\hat{J}^+_{\mathbf{1}}\hat{J}^-_{\mathbf{2}}+\hat{J}^-_{\mathbf{1}}\hat{J}^+_{\mathbf{2}} = 2(\hat{J}^x_{\mathbf{1}}\hat{J}^x_{\mathbf{2}}+\hat{J}^y_{\mathbf{1}}\hat{J}^y_{\mathbf{2}})$, $\hat{J}^+_{\mathbf{1}}\hat{J}^+_{\mathbf{2}}+\hat{J}^-_{\mathbf{1}}\hat{J}^-_{\mathbf{2}} = 2(\hat{J}^x_{\mathbf{1}}\hat{J}^x_{\mathbf{2}}-\hat{J}^y_{\mathbf{1}}\hat{J}^y_{\mathbf{2}})$, and $\hat{J}^+_{\boldsymbol{j}}+\hat{J}^-_{\boldsymbol{j}} = 2\hat{J}^x_{\boldsymbol{j}}$. If we set $J_{\rm H}=0$, $J'=0$, and $U'=U$ in Eq. (A25), we obtain

$$\begin{aligned}
(\hat{H}_{\rm eff})_{\mathbf{12}} =& -\frac{4}{9}\frac{t_{11}^2}{U}(\frac{5}{4}\hat{n}_{\mathbf{1}}\hat{n}_{\mathbf{2}}-\hat{\boldsymbol{J}}_{\mathbf{1}}\cdot\hat{\boldsymbol{J}}_{\mathbf{2}})\\
&-\frac{4}{9}\frac{t_{33}^2}{U}(\frac{5}{4}\hat{n}_{\mathbf{1}}\hat{n}_{\mathbf{2}}-\hat{\boldsymbol{J}}_{\mathbf{1}}\cdot\hat{\boldsymbol{J}}_{\mathbf{2}})+\frac{8}{9}\frac{t_{11}t_{33}}{U}(\frac{1}{4}\hat{n}_{\mathbf{1}}\hat{n}_{\mathbf{2}}+\hat{\boldsymbol{J}}_{\mathbf{1}}\cdot\hat{\boldsymbol{J}}_{\mathbf{2}})\\
&-\frac{16}{9}\frac{t_{\rm odd}^2}{U}(\frac{1}{2}\hat{n}_{\mathbf{1}}\hat{n}_{\mathbf{2}}+\hat{\boldsymbol{J}}_{\mathbf{1}}\cdot\hat{\boldsymbol{J}}_{\mathbf{2}}-2\hat{J}^y_{\mathbf{1}}\hat{J}^y_{\mathbf{2}})\\
&-\frac{16}{9}\frac{(t_{11}+t_{33})t_{\rm odd}}{U}(\hat{J}^x_{\mathbf{1}}\hat{J}^z_{\mathbf{2}}-\hat{J}^z_{\mathbf{1}}\hat{J}^x_{\mathbf{2}}).
\end{aligned}\tag{A26}$$

Next, we derive the terms of $(\hat{H}_{\rm eff})_{\mathbf{12}}$ for $\mathbf{2}-\mathbf{1}=(0,1)$. This derivation can be carried out in a similar way for

$\mathbf{2}-\mathbf{1}=(1,0)$ except the difference in the finite hopping integrals. The finite hopping integrals for $\mathbf{2}-\mathbf{1}=(0,1)$ come from the hopping integrals of $\hat{H}_0$ between the d_{yz} orbitals and between the d_{xy} orbitals ($-t_{11}$ and $-t_{33}$, respectively), and the hopping integrals of $\hat{H}_{\rm odd}$ between the d_{xz} orbital at $\mathbf{1}$ and the d_{xy} orbital at $\mathbf{2}$ and between the d_{xy} orbital at $\mathbf{1}$ and the d_{xz} orbital at $\mathbf{2}$ ($-t_{\rm odd}$ and $+t_{\rm odd}$, respectively). Carrying out similar calculations for $\mathbf{2}-\mathbf{1}=(1,0)$, we obtain the superexchange interactions for $\mathbf{2}-\mathbf{1}=(0,1)$:

$$
\begin{aligned}
(\hat{H}_{\rm eff})_{\mathbf{12}} =& -\frac{4}{27}\Big(\frac{t_{11}^2}{U+2J'}+\frac{2t_{11}^2}{U-J'}\Big)\Big(\frac{1}{4}\hat{n}_{\mathbf{1}}\hat{n}_{\mathbf{2}}-\hat{\boldsymbol{J}}_{\mathbf{1}}\cdot\hat{\boldsymbol{J}}_{\mathbf{2}}\Big)\\
&-\frac{4}{9}\frac{t_{11}^2}{U'-J_{\rm H}}\Big(\frac{3}{4}\hat{n}_{\mathbf{1}}\hat{n}_{\mathbf{2}}-\hat{J}_{\mathbf{1}}^x\hat{J}_{\mathbf{2}}^x\Big)-\frac{4}{9}\frac{t_{11}^2}{U'+J_{\rm H}}\Big(\frac{1}{4}\hat{n}_{\mathbf{1}}\hat{n}_{\mathbf{2}}+\hat{J}_{\mathbf{1}}^x\hat{J}_{\mathbf{2}}^x\Big)\\
&-\frac{4}{27}\Big(\frac{t_{33}^2}{U+2J'}+\frac{2t_{33}^2}{U-J'}\Big)\Big(\frac{1}{4}\hat{n}_{\mathbf{1}}\hat{n}_{\mathbf{2}}-\hat{\boldsymbol{J}}_{\mathbf{1}}\cdot\hat{\boldsymbol{J}}_{\mathbf{2}}\Big)\\
&-\frac{4}{9}\frac{t_{33}^2}{U'-J_{\rm H}}\Big(\frac{3}{4}\hat{n}_{\mathbf{1}}\hat{n}_{\mathbf{2}}-\hat{J}_{\mathbf{1}}^z\hat{J}_{\mathbf{2}}^z\Big)-\frac{4}{9}\frac{t_{33}^2}{U'+J_{\rm H}}\Big(\frac{1}{4}\hat{n}_{\mathbf{1}}\hat{n}_{\mathbf{2}}+\hat{J}_{\mathbf{1}}^z\hat{J}_{\mathbf{2}}^z\Big)\\
&-\frac{8}{27}\Big(\frac{t_{11}t_{33}}{U+2J'}-\frac{t_{11}t_{33}}{U-J'}\Big)\Big(\frac{1}{4}\hat{n}_{\mathbf{1}}\hat{n}_{\mathbf{2}}-\hat{\boldsymbol{J}}_{\mathbf{1}}\cdot\hat{\boldsymbol{J}}_{\mathbf{2}}\Big)\\
&+\frac{4}{9}\frac{t_{11}t_{33}}{U'-J_{\rm H}}\Big(\frac{1}{4}\hat{n}_{\mathbf{1}}\hat{n}_{\mathbf{2}}+\hat{\boldsymbol{J}}_{\mathbf{1}}\cdot\hat{\boldsymbol{J}}_{\mathbf{2}}+2\hat{J}_{\mathbf{1}}^y\hat{J}_{\mathbf{2}}^y\Big)\\
&+\frac{4}{9}\frac{t_{11}t_{33}}{U'+J_{\rm H}}\Big(\frac{1}{4}\hat{n}_{\mathbf{1}}\hat{n}_{\mathbf{2}}+\hat{\boldsymbol{J}}_{\mathbf{1}}\cdot\hat{\boldsymbol{J}}_{\mathbf{2}}-2\hat{J}_{\mathbf{1}}^y\hat{J}_{\mathbf{2}}^y\Big)\\
&-\frac{8}{27}\Big(\frac{2t_{\rm odd}^2}{U+2J'}+\frac{t_{\rm odd}^2}{U-J'}\Big)\Big(\frac{1}{4}\hat{n}_{\mathbf{1}}\hat{n}_{\mathbf{2}}+\hat{\boldsymbol{J}}_{\mathbf{1}}\cdot\hat{\boldsymbol{J}}_{\mathbf{2}}-2\hat{J}_{\mathbf{1}}^x\hat{J}_{\mathbf{2}}^x\Big)\\
&-\frac{4}{9}\frac{t_{\rm odd}^2}{U'-J_{\rm H}}\Big(\frac{5}{4}\hat{n}_{\mathbf{1}}\hat{n}_{\mathbf{2}}+2\hat{\boldsymbol{J}}_{\mathbf{1}}\cdot\hat{\boldsymbol{J}}_{\mathbf{2}}-5\hat{J}_{\mathbf{1}}^x\hat{J}_{\mathbf{2}}^x\Big)\\
&-\frac{4}{9}\frac{t_{\rm odd}^2}{U'+J_{\rm H}}\Big(\frac{1}{4}\hat{n}_{\mathbf{1}}\hat{n}_{\mathbf{2}}+\hat{J}_{\mathbf{1}}^x\hat{J}_{\mathbf{2}}^x\Big)\\
&-\frac{16}{27}\Big(\frac{t_{11}t_{\rm odd}}{U+2J'}-\frac{t_{11}t_{\rm odd}}{U-J'}\Big)\Big(\hat{J}_{\mathbf{1}}^y\hat{J}_{\mathbf{2}}^z-\hat{J}_{\mathbf{1}}^z\hat{J}_{\mathbf{2}}^y\Big)\\
&-\frac{16}{9}\frac{t_{11}t_{\rm odd}}{U'-J_{\rm H}}\Big(\hat{J}_{\mathbf{1}}^y\hat{J}_{\mathbf{2}}^z-\hat{J}_{\mathbf{1}}^z\hat{J}_{\mathbf{2}}^y\Big)\\
&-\frac{16}{27}\Big(\frac{t_{33}t_{\rm odd}}{U+2J'}+\frac{1}{2}\frac{t_{33}t_{\rm odd}}{U-J'}\Big)\Big(\hat{J}_{\mathbf{1}}^y\hat{J}_{\mathbf{2}}^z-\hat{J}_{\mathbf{1}}^z\hat{J}_{\mathbf{2}}^y\Big)\\
&-\frac{8}{9}\frac{t_{33}t_{\rm odd}}{U'-J_{\rm H}}\Big(\hat{J}_{\mathbf{1}}^y\hat{J}_{\mathbf{2}}^z-\hat{J}_{\mathbf{1}}^z\hat{J}_{\mathbf{2}}^y\Big). \qquad \text{(A27)}
\end{aligned}
$$

Because of the tetragonal symmetry of the system, Eq. (A27) is symbolically equivalent to Eq. (A25) after the replacements $\hat{J}_{\boldsymbol{j}}^x \to \hat{J}_{\boldsymbol{j}}^y$ and $\hat{J}_{\boldsymbol{j}}^y \to \hat{J}_{\boldsymbol{j}}^x$. Then, from Eqs. (A25) and (A27), we see that the energy difference between the in-plane and the out-of-plane alignments of the (π,π)-antiferromagnetic moments arises mainly from the difference between $\frac{8}{9}\frac{(t_{11})^2 J_{\rm H}}{(U')^2+(J_{\rm H})^2}[\sum_{\langle \boldsymbol{i},\boldsymbol{j}\rangle_x}\hat{J}_{\boldsymbol{i}}^y\hat{J}_{\boldsymbol{j}}^y+\sum_{\langle \boldsymbol{i},\boldsymbol{j}\rangle_y}\hat{J}_{\boldsymbol{i}}^x\hat{J}_{\boldsymbol{j}}^x]+\frac{16}{9}\frac{t_{11}t_{33}J_{\rm H}}{(U')^2+(J_{\rm H})^2}[\sum_{\langle \boldsymbol{i},\boldsymbol{j}\rangle_x}\hat{J}_{\boldsymbol{i}}^x\hat{J}_{\boldsymbol{j}}^x+\sum_{\langle \boldsymbol{i},\boldsymbol{j}\rangle_y}\hat{J}_{\boldsymbol{i}}^y\hat{J}_{\boldsymbol{j}}^y]$ and $\frac{8}{9}\frac{(t_{33})^2 J_{\rm H}}{(U')^2+(J_{\rm H})^2}\sum_{\langle \boldsymbol{i},\boldsymbol{j}\rangle}\hat{J}_{\boldsymbol{i}}^z\hat{J}_{\boldsymbol{j}}^z$, as described in Sec. IV. For $J_{\rm H}=0$, $J'=0$, and $U'=U$, Eq. (A27) reduces to the following equation:

$$
\begin{aligned}
(\hat{H}_{\rm eff})_{\mathbf{12}} =& -\frac{4}{9}\frac{t_{11}^2}{U}\Big(\frac{5}{4}\hat{n}_{\mathbf{1}}\hat{n}_{\mathbf{2}}-\hat{\boldsymbol{J}}_{\mathbf{1}}\cdot\hat{\boldsymbol{J}}_{\mathbf{2}}\Big)\\
&-\frac{4}{9}\frac{t_{33}^2}{U}\Big(\frac{5}{4}\hat{n}_{\mathbf{1}}\hat{n}_{\mathbf{2}}-\hat{\boldsymbol{J}}_{\mathbf{1}}\cdot\hat{\boldsymbol{J}}_{\mathbf{2}}\Big)\\
&+\frac{8}{9}\frac{t_{11}t_{33}}{U}\Big(\frac{1}{4}\hat{n}_{\mathbf{1}}\hat{n}_{\mathbf{2}}+\hat{\boldsymbol{J}}_{\mathbf{1}}\cdot\hat{\boldsymbol{J}}_{\mathbf{2}}\Big)\\
&-\frac{16}{9}\frac{t_{\rm odd}^2}{U}\Big(\frac{1}{2}\hat{n}_{\mathbf{1}}\hat{n}_{\mathbf{2}}+\hat{\boldsymbol{J}}_{\mathbf{1}}\cdot\hat{\boldsymbol{J}}_{\mathbf{2}}-2\hat{J}_{\mathbf{1}}^x\hat{J}_{\mathbf{2}}^x\Big)\\
&-\frac{16}{9}\frac{(t_{11}+t_{33})t_{\rm odd}}{U}\Big(\hat{J}_{\mathbf{1}}^y\hat{J}_{\mathbf{2}}^z-\hat{J}_{\mathbf{1}}^z\hat{J}_{\mathbf{2}}^y\Big). \qquad \text{(A28)}
\end{aligned}
$$

Moreover, we can derive the terms of $(\hat{H}_{\rm eff})_{\mathbf{12}}$ for $\mathbf{2}-\mathbf{1}=(1,1)$ and $(1,-1)$. Those derivations are simpler than the derivations for $\mathbf{2}-\mathbf{1}=(1,0)$ and $(0,1)$ because the finite hopping integrals for $\mathbf{2}-\mathbf{1}=(1,\pm1)$ are the hopping integrals between the d_{xz} orbital and the d_{yz} orbital, $\mp t'_{12}$, and the hopping integral between the d_{xy} orbitals, $-t'_{33}$. The results for $\mathbf{2}-\mathbf{1}=(1,1)$ and $(1,-1)$ are

$$
\begin{aligned}
(\hat{H}_{\rm eff})_{\mathbf{12}} =& -\frac{8}{9}\frac{(t'_{12})^2}{U-J'}\Big(\frac{1}{4}\hat{n}_{\mathbf{1}}\hat{n}_{\mathbf{2}}+\hat{\boldsymbol{J}}_{\mathbf{1}}\cdot\hat{\boldsymbol{J}}_{\mathbf{2}}-2\hat{J}_{\mathbf{1}}^z\cdot\hat{J}_{\mathbf{2}}^z\Big)\\
&-\frac{4}{9}\frac{(t'_{12})^2}{U'-J_{\rm H}}\Big(\frac{7}{4}\hat{n}_{\mathbf{1}}\hat{n}_{\mathbf{2}}+3\hat{J}_{\mathbf{1}}^z\hat{J}_{\mathbf{2}}^z\Big)\\
&-\frac{4}{9}\frac{(t'_{12})^2}{U'+J_{\rm H}}\Big(\frac{3}{4}\hat{n}_{\mathbf{1}}\hat{n}_{\mathbf{2}}-2\hat{\boldsymbol{J}}_{\mathbf{1}}\cdot\hat{\boldsymbol{J}}_{\mathbf{2}}+\hat{J}_{\mathbf{1}}^z\hat{J}_{\mathbf{2}}^z\Big)\\
&-\frac{4}{27}\Big(\frac{(t'_{33})^2}{U+2J'}+\frac{2(t'_{33})^2}{U-J'}\Big)\Big(\frac{1}{4}\hat{n}_{\mathbf{1}}\hat{n}_{\mathbf{2}}-\hat{\boldsymbol{J}}_{\mathbf{1}}\cdot\hat{\boldsymbol{J}}_{\mathbf{2}}\Big)\\
&-\frac{4}{9}\frac{(t'_{33})^2}{U'-J_{\rm H}}\Big(\frac{3}{4}\hat{n}_{\mathbf{1}}\hat{n}_{\mathbf{2}}-\hat{J}_{\mathbf{1}}^z\hat{J}_{\mathbf{2}}^z\Big)\\
&-\frac{4}{9}\frac{(t'_{33})^2}{U'+J_{\rm H}}\Big(\frac{1}{4}\hat{n}_{\mathbf{1}}\hat{n}_{\mathbf{2}}+\hat{J}_{\mathbf{1}}^z\hat{J}_{\mathbf{2}}^z\Big)\\
&-\frac{8}{9}\frac{t'_{12}t'_{33}}{U'-J_{\rm H}}\Big(\hat{J}_{\mathbf{1}}^x\hat{J}_{\mathbf{2}}^y+\hat{J}_{\mathbf{1}}^y\hat{J}_{\mathbf{2}}^x\Big)\\
&+\frac{8}{9}\frac{t'_{12}t'_{33}}{U'+J_{\rm H}}\Big(\hat{J}_{\mathbf{1}}^x\hat{J}_{\mathbf{2}}^y+\hat{J}_{\mathbf{1}}^y\hat{J}_{\mathbf{2}}^x\Big), \qquad \text{(A29)}
\end{aligned}
$$

and

$$
\begin{aligned}
(\hat{H}_{\rm eff})_{\mathbf{12}} =& -\frac{8}{9}\frac{(t'_{12})^2}{U-J'}(\frac{1}{4}\hat{n}_{\mathbf{1}}\hat{n}_{\mathbf{2}}+\hat{\boldsymbol{J}}_{\mathbf{1}}\cdot\hat{\boldsymbol{J}}_{\mathbf{2}}-2\hat{J}^z_{\mathbf{1}}\cdot\hat{J}^z_{\mathbf{2}})\\
&-\frac{4}{9}\frac{(t'_{12})^2}{U'-J_{\rm H}}(\frac{7}{4}\hat{n}_{\mathbf{1}}\hat{n}_{\mathbf{2}}+3\hat{J}^z_{\mathbf{1}}\hat{J}^z_{\mathbf{2}})\\
&-\frac{4}{9}\frac{(t'_{12})^2}{U'+J_{\rm H}}(\frac{3}{4}\hat{n}_{\mathbf{1}}\hat{n}_{\mathbf{2}}-2\hat{\boldsymbol{J}}_{\mathbf{1}}\cdot\hat{\boldsymbol{J}}_{\mathbf{2}}+\hat{J}^z_{\mathbf{1}}\hat{J}^z_{\mathbf{2}})\\
&-\frac{4}{27}(\frac{(t'_{33})^2}{U+2J'}+\frac{2(t'_{33})^2}{U-J'})(\frac{1}{4}\hat{n}_{\mathbf{1}}\hat{n}_{\mathbf{2}}-\hat{\boldsymbol{J}}_{\mathbf{1}}\cdot\hat{\boldsymbol{J}}_{\mathbf{2}})\\
&-\frac{4}{9}\frac{(t'_{33})^2}{U'-J_{\rm H}}(\frac{3}{4}\hat{n}_{\mathbf{1}}\hat{n}_{\mathbf{2}}-\hat{J}^z_{\mathbf{1}}\hat{J}^z_{\mathbf{2}})\\
&-\frac{4}{9}\frac{(t'_{33})^2}{U'+J_{\rm H}}(\frac{1}{4}\hat{n}_{\mathbf{1}}\hat{n}_{\mathbf{2}}+\hat{J}^z_{\mathbf{1}}\hat{J}^z_{\mathbf{2}})\\
&+\frac{8}{9}\frac{t'_{12}t'_{33}}{U'-J_{\rm H}}(\hat{J}^x_{\mathbf{1}}\hat{J}^y_{\mathbf{2}}+\hat{J}^y_{\mathbf{1}}\hat{J}^x_{\mathbf{2}})\\
&-\frac{8}{9}\frac{t'_{12}t'_{33}}{U'+J_{\rm H}}(\hat{J}^x_{\mathbf{1}}\hat{J}^y_{\mathbf{2}}+\hat{J}^y_{\mathbf{1}}\hat{J}^x_{\mathbf{2}}),
\end{aligned}
\tag{A30}
$$

respectively. In particular, for $J_{\rm H}=0$, $J'=0$, and $U'=U$, $(\hat{H}_{\rm eff})_{\mathbf{12}}$ for $\mathbf{2}-\mathbf{1}=(1,\pm1)$ becomes

$$
(\hat{H}_{\rm eff})_{\mathbf{12}} = -\frac{4}{3}\frac{(t'_{12})^2}{U}\hat{n}_{\mathbf{1}}\hat{n}_{\mathbf{2}}-\frac{4}{9}\frac{(t'_{33})^2}{U}(\frac{5}{4}\hat{n}_{\mathbf{1}}\hat{n}_{\mathbf{2}}-\hat{\boldsymbol{J}}_{\mathbf{1}}\cdot\hat{\boldsymbol{J}}_{\mathbf{2}}). \tag{A31}
$$

Combining Eqs. (A26), (A28), and (A31) together and neglecting the product terms of the hole-density operators, we finally obtain Eq. (6).

Appendix B: Derivation of Eq. (11)

In this appendix, I derive Eq. (11). The derivation consists of three steps.

First, we rewrite $\hat{H}_{\rm eff}$ in Eq. (11) as

$$
\hat{H}_{\rm eff}=\sum_{\boldsymbol{i},\boldsymbol{j}}\sum_{\alpha,\beta=x,y,z}J^{\alpha\beta}_{\boldsymbol{j}\boldsymbol{i}}\hat{J}^{\beta}_{\boldsymbol{i}}\hat{J}^{\alpha}_{\boldsymbol{j}}, \tag{B1}
$$

where $\sum_{\boldsymbol{i},\boldsymbol{j}}$ is the summations of $\boldsymbol{i}$ and $\boldsymbol{j}$ for all N sites. From Eq. (6), we can explicitly write down $J^{\alpha\beta}_{\boldsymbol{j}\boldsymbol{i}}$ by recalling $t^{(\rm even)}_{ab;\boldsymbol{i}\boldsymbol{j}}=t^{(\rm even)}_{ab;\boldsymbol{j}\boldsymbol{i}}$, $t^{(\rm odd)}_{ab;\boldsymbol{i}\boldsymbol{j}}=-t^{(\rm odd)}_{ab;\boldsymbol{j}\boldsymbol{i}}$, $\sum_{\langle\boldsymbol{i},\boldsymbol{j}\rangle_x}\cdots=\frac{1}{2}\sum_{\boldsymbol{i},\boldsymbol{j}}\cdots$, $\sum_{\langle\boldsymbol{i},\boldsymbol{j}\rangle_y}\cdots=\frac{1}{2}\sum_{\boldsymbol{i},\boldsymbol{j}}\cdots$, and $\sum_{\langle\langle\boldsymbol{i},\boldsymbol{j}\rangle\rangle}\cdots=\sum_{\boldsymbol{i},\boldsymbol{j}}\cdots$. For example, $J^{\alpha\beta}_{\boldsymbol{j}\boldsymbol{i}}$ for $\boldsymbol{j}-\boldsymbol{i}=(\pm1,0)$ and $\alpha=\beta=x$ is $\frac{1}{2}(J_0-J_{\rm odd})$; $J^{\alpha\beta}_{\boldsymbol{j}\boldsymbol{i}}$ for $\boldsymbol{j}-\boldsymbol{i}=(0,\pm1)$, $\alpha=z$, and $\beta=y$ is $\mp\frac{1}{2}D$; $J^{\alpha\beta}_{\boldsymbol{j}\boldsymbol{i}}$ for $\boldsymbol{j}-\boldsymbol{i}=(\pm1,\pm1)$ and $\alpha=\beta=z$ is J_2.

Second, we apply the mean-field approximation (for example see Ref. 11) to Eq. (B1) by using $\hat{J}^{\alpha}_{\boldsymbol{j}}\approx\langle\hat{J}^{\alpha}_{\boldsymbol{j}}\rangle$, and derive the energy at absolute zero of temperature in order to determine the ground state. As a result, the energy is given by

$$
\langle\hat{H}_{\rm eff}\rangle=\sum_{\boldsymbol{i},\boldsymbol{j}}\sum_{\alpha,\beta=x,y,z}J^{\alpha\beta}_{\boldsymbol{j}\boldsymbol{i}}\langle\hat{J}^{\beta}_{\boldsymbol{i}}\rangle\langle\hat{J}^{\alpha}_{\boldsymbol{j}}\rangle. \tag{B2}
$$

Since the mean-field approximation neglects the fluctuations, the magnitude of $\langle\hat{J}^{\alpha}_{\boldsymbol{j}}\rangle$ should be equal to $J=\frac{1}{2}$ for all N sites. Namely, $\langle\hat{J}^{\alpha}_{\boldsymbol{j}}\rangle$ in Eq. (B2) should satisfy the hard-pseudospin constraints,

$$
\frac{1}{4}=\frac{1}{N}\sum_{\boldsymbol{i}}\sum_{\alpha}|\langle\hat{J}^{\alpha}_{\boldsymbol{i}}\rangle|^2. \tag{B3}
$$

Third, by using the Fourier transformation of $\langle\hat{J}^{\alpha}_{\boldsymbol{j}}\rangle$, we can rewrite $\langle\hat{H}_{\rm eff}\rangle$ in a quadratic form, Eq. (11), with Eqs. (13)–(19). In addition, we can rewrite Eq. (B3) as Eq. (12). After determining the lowest eigenvalue of Eq. (11), we should check whether the eigenvector satisfies Eq. (12).

* Electronic address: arakawa@hosi.phys.s.u-tokyo.ac.jp

1 T. Kimura, T. Goto, H. Shintani, K. Ishizaka, T. Arima, and Y. Tokura, Nature (London) **426**, 55 (2003).
2 H. Katsura, N. Nagaosa, and A. V. Balatsky, Phys. Rev. Lett. **95**, 057205 (2005).
3 I. A. Sergienko and E. Dagotto, Phys. Rev. B **73**, 094434 (2006).
4 H. J. Xiang, S.-H. Wei, M.-H. Whangbo, and J. L. F. Da Silva, Phys. Rev. Lett. **101**, 037209 (2008).
5 Y. Machida, S. Nakatsuji, S. Onoda, T. Tayama, and T. Sakakibara, Nature (London) **463**, 210 (2009).
6 M. Udagawa and R. Moessner, Phys. Rev. Lett. **111**, 036602 (2013).
7 S. Seki, X. Z. Yu, S. Ishiwata, and Y. Tokura, Science **336**, 198 (2012).
8 M. Udagawa and Y. Motome, Phys. Rev. Lett. **104**, 106409 (2010).
9 I. Dzyaloshinsky, J. Phys. Chem. Solids **4**, 241 (1958).
10 T. Moriya, Phys. Rev. Lett. **4**, 228 (1960).
11 A. Yoshimori, J. Phys. Soc. Jpn. **14**, 807 (1959).
12 Y. Tokura and N. Nagaosa, Science **288**, 462 (2000).
13 G. Chen and L. Balents, Phys. Rev. B **78**, 094403 (2008).
14 R. Shindou, Phys. Rev. B **93**, 094419 (2016).
15 T. Mizoguchi, K. Hwang, E. K.-H. Lee, and Y. B. Kim, Phys. Rev. B **94**, 064416 (2016).
16 A. Biffin, R. D. Johnson, S. Choi, F. Freund, S. Manni, A. Bombardi, P. Manuel, P. Gegenwart, and R. Coldea, Phys. Rev. B **90**, 205116 (2014).

[17] J. G. Rau, Eric Kin-Ho Lee, and Hae-Young Kee, Phys. Rev. Lett. **112**, 077204 (2014).

[18] E. K.-H. Lee, J. G. Rau, and Y. B. Kim, Phys. Rev. B **93**, 184420 (2016).

[19] B. J. Kim, H. Jin, S. J. Moon, J.-Y. Kim, B.-G. Park, C. S. Leem, Jaejun Yu, T. W. Noh, C. Kim, S.-J. Oh, J.-H. Park, V. Durairaj, G. Cao, and E. Rotenberg, Phys. Rev. Lett. **101**, 076402 (2008).

[20] B. J. Kim, H. Ohsumi, T. Komesu, S. Sakai, T. Morita, H. Takagi, and T. Arima, Science **323**, 1329 (2009).

[21] A. Kitaev, Ann. Phys. **321**, 2 (2006).

[22] Y. Yanase, J. Phys. Soc. Jpn. **82**, 044711 (2013).

[23] T. Mizoguchi and N. Arakawa, Phys. Rev. B **93**, 041304(R) (2016).

[24] P. W. Anderson, Phys. Rev. **115**, 2 (1959).

[25] K. I. Kugel and D. I. Khomskii, Zh. Eksp. Teor. Fiz. **64**, 1429 (1973) [Sov. Phys. JETP **37**, 725 (1973)].

[26] S. Ishihara, T. Hatakeyama, and S. Maekawa, Phys. Rev. B **65**, 064442 (2002).

[27] G. Jackeli and G. Khaliullin, Phys. Rev. Lett. **102**, 017205 (2009).

[28] H. Kamimura, S. Sugano, and Y. Tanabe, *Ligand field theory and its applications* (Syōkabō, Tokyo, 1969).

[29] H. Watanabe, T. Shirakawa, and S. Yunoki, Phys. Rev. Lett. **105**, 216410 (2010).

[30] J. M. Luttinger and L. Tisza, Phys. Rev. **70**, 954 (1946).

[31] Y. Nakamura and Y. Yanase, J. Phys. Soc. Jpn. **82**, 083705 (2013).

[32] G. Cao, J. Bolivar, S. McCall, J. E. Crow, and R. P. Guertin, Phys. Rev. B **57**, R11 039 (1998).

[33] M. K. Crawford, M. A. Subramanian, R. L. Harlow, J. A. Fernandez-Baca, Z. R. Wang, and D. C. Johnston, Phys. Rev. B **49**, 9198 (1994).

[34] Q. Huang, J. L. Soubeyroux, O. Chmaissem, I. Natali Sora, A. Santoro, R. J. Cava, J. J. Krajewski, W. F. Peck Jr., J. Solid State Chem. **112**, 355 (1994).